

Thermal peak load shaving through users request variations

*Original*

Thermal peak load shaving through users request variations / Verda, V., Guelpa, E., Sciacovelli, A., Acquaviva, A., Patti, E.. - In: INTERNATIONAL JOURNAL OF THERMODYNAMICS. - ISSN 2146-1511. - 19:3(2016), pp. 168-176.  
[10.5541/ijot.5000175955]

*Availability:*

This version is available at: 11583/2650737 since: 2018-03-02T15:09:58Z

*Publisher:*

DergiPark

*Published*

DOI:10.5541/ijot.5000175955

*Terms of use:*

This article is made available under terms and conditions as specified in the corresponding bibliographic description in the repository

*Publisher copyright*

(Article begins on next page)

## Thermal Peak Load Shaving Through Users Request Variations in District Heating Systems

Verda V<sup>1,\*</sup>, Guelpa E<sup>2</sup>, Sciacovelli A<sup>3</sup>, Acquaviva A.<sup>4</sup>, Patti E.<sup>5</sup>

Politecnico di Torino Dipartimento Energia, Torino, Italy  
E-mail: <sup>1</sup>vittorio.verda@polito.it, <sup>2</sup>elisa.guelpa@polito.it,  
School of Chemical Engineering – Birmingham Centre for Energy Storage (BCES)  
E-mail: <sup>3</sup>a.sciacovelli@bham.ac.uk  
Politecnico di Torino Dipartimento di Automatica e Informatica, Torino, Italy  
E-mail: <sup>4</sup>andrea.acquaviva@polito.it, <sup>5</sup>edoardo.patti@polito.it,

Received 08 February 2016, Revised 29 July 2016, Accepted 01 August 2016

### Abstract

Peak shaving is a relatively new approach aimed at increasing the primary energy efficiency in District Heating Systems. This is mainly performed using thermal storage units that can be charged when the thermal request is small, usually at night, and discharged to cover peak requests. Thermal storage typically allows one increasing the utilization of waste heat, renewables and cogeneration systems while reducing the use of boilers. An alternative option to conventional thermal storage is “virtual storage”. This consists in modifying the thermal request profiles of buildings in order to reduce their contributions in peak hours. Such modifications rely on the thermal capacity of buildings in order to comply with end-user requirements on the internal temperatures. The analysis of possible operational strategies should be performed using an integrated simulation, which considers both the thermos-fluid dynamic behavior of the network and the thermal behavior of the buildings. In this paper, a physical tool specifically conceived for the analysis of peak shaving in large networks through virtual storage is presented and applied to a portion of the Turin district heating network. Detailed information about thermal requests of buildings obtained from a pervasive metering system is used in order to characterize their behavior. This piece of information is then adopted for constraining and checking possible different operational strategies. Two different scenarios are analyzed and compared with current operation in terms of primary energy consumption, showing that primary energy savings of the order of 5% can be achieved without affecting the comfort perceived by the users.

**Keywords:** District heating operation; thermal fluid dynamic model; building request; virtual thermal storage.

### 1. Introduction

During last decades, District Heating Systems (DHS) technology has gained in importance because of the possibility to integrate waste heat available from industrial processes and heat generated from high efficiency cogeneration plants and renewable energy plants [1]. This allows one to achieve significant decrease in the fuel consumption associated with the thermal request of buildings and, consequently, to reduce carbon emissions. To provide a quantification of the possible advantages in terms of primary energy consumption and the potential margins for improvement, the Turin district heating network is considered in this work.

The Turin district heating network is the largest network in Italy and one of the largest in Europe. Currently the network provides heating to about 5700 buildings for a total volume of 58 million m<sup>3</sup>, while hot water is supplied to about 10% of the users. [2]. An expansion of the system to connect additional 16 million cubic meters of buildings is already planned

The network is constituted by 528 km of double pipeline. The water supply temperature is maintained constant at about 120°C during the winter season while it is reduced summer. The return temperature is about 65°C during usual daily operation, but varies significantly

depending on the thermal load. The entire network can be considered as composed by two parts, which are directly connected: the transport network and the distribution networks. The transport network is constituted by the pipes with larger diameter, (usually larger than 200 mm). This network connects the thermal plants to the distribution networks. Each distribution network supplies water to a group of buildings that are located in the same area. In the Turin network there are 182 distribution networks. Figure 1 shows the transport network and, in detail, three distribution networks. The transport network includes some loops, in order to limit possible effects of failures and to allow better flow distribution. In contrast the distribution networks are usually tree-shaped networks, although some of them present loops as well. Because of the large extension and the presence of various loops, solution of the fluid flow in the network is not trivial and efficient algorithms are necessary.

To comply with the thermal request, six thermal plants located in different areas are connected with the network. A description of the plants and their characteristics are reported in Table 1. The maximum load is about 1.3 GW, while the annual thermal load is about 2000 GWh. Three cogeneration plants are able to cover the thermal load up to 740 MW. When the load exceeds this value the storage

systems are discharged providing a thermal power of up to about 270 MW for a limited time period. These units have a total capacity of 12500 m<sup>3</sup> and are charged at night, when the request is smaller than the installed cogeneration capacity, as it can be noticed from the thermal load curve shown in Figure 2. This means that storage units virtually expand the cogeneration capacity, increasing the annual amount of heat and reducing the use of boilers. Operational data report that during the heating season 2013-14 storage units have supplied about 0.18 GWh of heat, allowing more than 95% of heat production from cogeneration. Due to the continuous expansion of the network, a larger storage capacity is planned. When the load exceeds about 1000 MW the boilers operate.

Table 1. Characteristics of the thermal plants.

Plant	Type	Nominal Power [MW]
Torino Nord	Cogeneration	220
	Boilers	340
	Storage	150
Moncalieri	2 Cogeneration plants	520
	Boilers	141
Politecnico	Boilers	255
	Storage	60
Martinetto	Storage	60
	BIT	255
Mirafiori Nord	Boilers	35

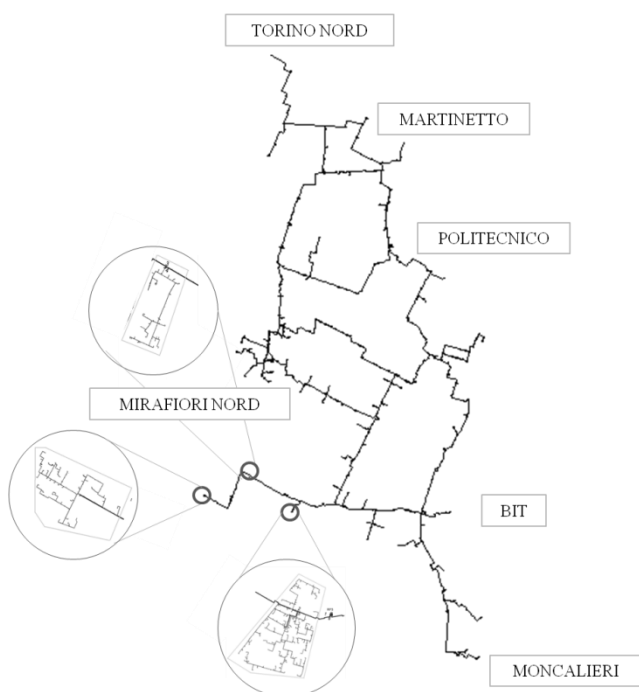


Figure 1. Schematic of Turin District Heating Network: transport network thermal plants and three distribution networks.

In urban areas it is not always possible (or economically convenient) to find proper locations where storage units can be installed, therefore alternative options for thermal peak

shaving are investigated, such as distributed storage units [3] and variation in the thermal request of users (virtual storage) [4].

Recent works in literature demonstrate the large interest in increasing exploitation of cogeneration, renewable sources and storage technologies. In [5] a model for optimizing integration of boilers, heat pumps and cogeneration is proposed. The possibility of using a dynamic simulation tool with the aim of studying interactions of cogeneration heat pump/district heating network, with a particular emphasis on the network to heat storage capacity, is examined in [6]. In [7] the use of storage systems that are charged at night and used during the start-up transients is examined for peak-shaving purpose. This is shown to be a very effective measure for reducing the boiler utilization and enhance cogeneration. In [4] and [8], two different approaches are used to analyze the opportunities to modify the thermal request profile of some users in order to maximize heat production from cogeneration or renewable plants. The approach in [4] is mainly focused on the network modeling, while a very compact approach for the analysis of buildings is adopted. In contrast, in [8] a more accurate model of buildings is proposed, but this forces the application to a limited number of buildings.

Investigations on system responses to variations in plant configurations (e.g. installation of storage units) or in user request should be performed using numerical models of the district heating network in order to relate the thermal request of users to the heat production. This is the reason why district heating modeling have been largely applied both at design [9] and operation stages [10]. Thermo-fluid dynamic modeling represents a valuable approach in order to quantify the thermal peak variation when some changes are applied to the DHS.

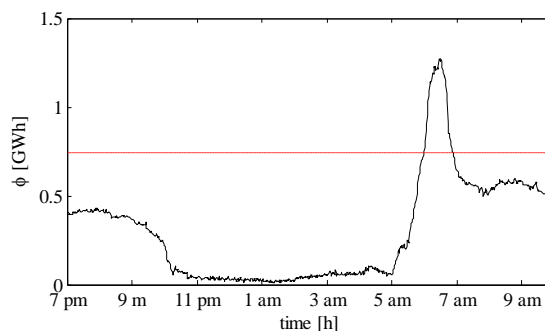


Figure 2. Global thermal request in a late winter day in the Turin DHS.

This paper starts from the approach proposed in [4] and emphasizes the use of compact models of buildings while performing the analysis of district heating networks. The characteristic parameters of the various buildings are extracted from measurements operated at the heat exchangers, which allow massive applications to large networks. In fact, parameters can be easily extracted for a large number of buildings and the model can be then integrated in the network simulations.

The model results of a single building are compared with internal temperature measurements in order to show that it is suitable for the analysis of variations in the thermal load profile. An application to a distribution network supplying heat to 104 buildings is presented. Two scenarios obtained by modifying the thermal request profiles of buildings but without lowering the daytime internal

temperatures are analyzed in terms of primary energy consumption.

## 2. Methodology

### 2.1 Physical Models

Two models have been developed for the analysis of possible variations in the thermal request profiles of buildings: a compact building model and the thermo-fluid dynamic model of the network. The network model has been used in order to analyze how perturbations in the thermal requests affect the global heat load at the distribution network. These models are fully integrated and perform the following analysis, which is here presented as decomposed in phases although it is obtained in a single step: 1) the start-up and shut-down time schedule of the various buildings is set; 2) simulation of the supply network is performed to obtain the temperature of water entering the heat exchanger in each building; 3) using the building model the internal temperature in the building and the temperature of water exiting the heat exchanger are calculated; 4) simulation of the return network using the temperatures of water exiting the heat exchanger as the boundary conditions is performed in order to obtain the temperature of water returning at the thermal plants; 5) the thermal load and the corresponding primary energy consumption are calculated.

#### 2.1.1 Building Model

The building model includes the thermal substation and the “macro heating device” which represents the conjunction of the heating system and the building envelope. A schematic of the system considered to simulate the buildings is shown in Figure 3.

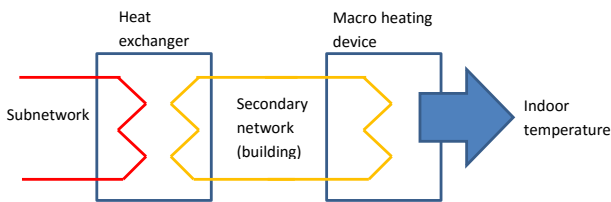


Figure 3. Schematic of the heating system in the buildings.

An energy balance of the building is written including the unsteady term, the heat provided by the heating system and the losses with the environment, namely

$$\Phi_{syst} + \Phi_{losses} = Mc \frac{dT}{dt} \quad (1)$$

This means that a single average temperature  $T$  is considered in the building. For the purpose of the analysis proposed in this work, this does not represent a limitation of the model as it is discussed in the next section. Losses can be expressed through a global dispersion coefficient per unit volume  $U_{vol}$ :

$$\Phi_{losses} = U_{vol}V(T - T_{outside}) \quad (2)$$

Both parameters  $Mc$  and  $U_{vol}V$  are evaluated through the analysis of experimental data available at each heat exchanger. These are the four temperatures at the heat exchanger, the mass flow rate on the primary network and the external temperature. The term  $U_{vol}V$  is evaluated using data collected when the system is operating in pseudo

steady-state conditions, which typically take place in the afternoon. In these conditions, Eq. (1) is rewritten as:

$$U_{vol}V = \frac{\Phi_{syst}}{(T - T_{outside})} \quad (3)$$

The term  $Mc$  has been evaluated considering the transient operation after the heating system is switched off. In this case, it is assumed that when the temperature of water exiting the heat exchanger on the secondary side of the heating system is approaching the indoor temperature, these two temperatures tend to decrease in a similar way. Therefore, data collected during the last stage of the water cooling can be used to evaluate the decrease in the internal temperature and thus the thermal capacity of the building:

$$Mc = U_{vol}V(T - T_{outside}) \cdot \frac{dt}{dT} \quad (4)$$

Temperatures of the water exiting the DHS heat exchangers at the secondary side,  $T_{out\_sec}$ , and heat flow exchange at the users,  $\Phi_{syst}$ , are evaluated using the substation model.

The heating system of each building has been modeled considering two heat exchangers. The first heat exchanger is the one in the substation where district heating network water flows on the primary side and the water of the building heating system flows on the secondary side. The second heat exchanger simulates the heating devices in the building as a single component exchanging heat with the indoor environments. The heat exchangers are modeled using an effectiveness-NTU method. A time delay is considered in order to account for the average time requested for water circulation on the secondary network. This is a third parameter that characterizes the building and it is evaluated through comparison of the calculated thermal request profile and the registered evolution.

Temperatures on the secondary network have been calculated at each time step, since these values vary during operation. In contrast, the mass flow rate on the secondary network is constant when the heating system is operating, since typically no variable speed pumps are installed in the buildings. The mass flow rate on the secondary network is zero when the heating system is not operating.

#### 2.1.2 Network Model

The network model is used in order to take into account for the effects of the long distances involved in the network on temperature distribution. In fact, on the supply network, temperature reduces while water flow from the plants towards the buildings because of heat losses. On the return network, water exiting the heat exchangers in the buildings flows on the return distribution network and mixes with the various streams coming from the users located in the other areas. These streams are at different temperatures, due to the different distance of the users. Thermal losses also affect temperature distribution, even if these are much smaller in the return network. As a result of these effects, temperature evolution at the plants is significantly different than that at the users, therefore the thermal load profile is different than the summation of the thermal request profiles of the buildings.

A one dimensional model has been applied to the analysis of the thermo-fluid dynamic behavior of the district heating network. Network topology is handled using a graph approach [11]. Each pipe of the network is

considered as a branch starting and ending with two nodes, conventionally assumed as the inlet and outlet sections, respectively. In this way mass flow rate assumes positive values when water flows from the conventional inlet to the outlet sections and negative values otherwise. The incidence matrix  $A$  is used in order to describe the network topology by expressing the connections between nodes and branches. Matrix  $A$  has as many rows as the number of nodes and as many columns as the number of branches. The general element  $A_{ij}$  is equal to 1 or -1 if the branch  $j$  enters or exits the node  $i$  and 0 otherwise. The fluid-dynamic model considers the mass conservation equation applied to all the nodes and the momentum conservation equation applied to all the branches. These equations are here considered in steady state form, since fluid-dynamic perturbations travel the entire network in a period of time smaller than the time step adopted for calculations (60 s).

In this specific application, the fluid flow is solved separately for the supply and return network. This is performed in order to obtain a direct link between the model and the mass flow rates measured at the substations. Mass flow rates are imposed as the boundary conditions in the outlet sections of the supply network, i.e. at the heat exchangers in each building, and in the inlet sections of the return network. Mass flow rates are also imposed in the nodes corresponding with the thermal plants, thus providing the production level of each plant, with the exception of the Moncalieri plant, where the master pressurizing system is located. This system imposes a fix reference pressure level for the entire network (about 9 bar). Pressure in the node corresponding to the inlet section of the supply network is set to a proper value so that water properly circulates in the network. This pressure increases with increasing mass flow rate circulating, up to a value of about 16 bar. Pressure in the outlet section of the return network is maintained to a value higher than 2.5 bar in order to prevent from water evaporation in all points of the network despite the variation in elevation. The solution of the mass and momentum equations is performed using a SIMPLE (semi implicit method for pressure linked equation) algorithm [12]. It is a guess and correction method: at the beginning a pressure vector is guessed and, during the iterations, pressure and mass flow rate vectors are corrected.

The thermal model is obtained expressing the energy equation in control volumes centered at the nodes. An Upwind scheme [13] is adopted in order to express the temperatures at the control surfaces as the function of the temperatures at the nodes. Energy equation is considered in transient form since thermal perturbations travel the network at the water velocity, which is the order of few meters per second, depending on the thermal request and the portion of network. Velocity is typically small at night and in the distribution networks, therefore temperature variations in these conditions take a lot of time, easily of the order of hours, to reach the thermal plants. As far as boundary conditions is concerned, temperature is imposed at the inlet nodes, i.e. the nodes corresponding with the thermal plants on the supply network and the nodes corresponding to the outlet section of the heat exchangers in the return network. No boundary conditions are imposed on the outlet nodes, but proper energy balances are written instead.

Further details on the numerical method are available in [14]. In [15] this model was applied to the Turin transport network in order to obtain the return temperatures at the

thermal plants as the function of time. Using these temperatures, the total thermal load of the plants was calculated and compared with the available measurements for validation purpose. Results show that the modeling approach is able to capture with sufficient precision the thermal load variation during a period of 14 hours which was including the night load reduction and the morning peak.



Figure 4. Schematic of the selected distribution network.

### 2.3 Approach Description

The total thermal load  $\Phi$  is calculated as:

$$\Phi = \sum_{i=1}^{nt} G_i \cdot c \cdot (T_{\text{sup}} - T_{\text{ret}_i}) \quad (5)$$

where  $nt$  is the number of operating plants,  $G_i$  is the mass flow rate at each plant,  $T_{\text{sup}}$  is the supply temperature (which is almost constant and similar for all plants) and  $T_{\text{ret}_i}$  is the return temperature at each plant.

As shown in Figure 2, the total thermal load presents a peak at about 6 a.m., which cannot be directly covered using cogeneration systems only. Despite the availability of thermal storage units, about 300 MW are covered using boilers, therefore additional options that allow enhancing the use of cogeneration are investigated, with the aim of reducing the primary energy cost of heat supplied to the buildings.

This peak has two causes: 1) mass flow rate in the morning, when most users turn the heating system on, increases significantly. As the propagation time of fluid dynamic disturbances in the network is fast, this effect is perceived at the thermal plants almost instantaneously; 2) due to the large variation in the thermal request, temperature on the return network presents large variations. These variations travel the network at the fluid velocity,

thus reach the plants (affecting the return temperature  $T_{ret,i}$ ) with time delays which depend on the distance between users and plants as well as on the thermal request.

In the case of typical winter days, the peak is similar in shape and magnitude to the one shown the figure. The main difference in the load curve is associated with the off-peak request, which strictly depends on the external temperatures.

In this analysis, one of the distribution networks has been considered in order to analyze possible effects that can be achieved in terms of total load variation through changes in the thermal request of single buildings. Network topology is shown in Figure 4. This network connects the transport network to 104 buildings located in the central zone, close to the Politecnico plant. The total volume of buildings connected with this distribution network is about 630000 m<sup>3</sup>, which means slightly more than 1% of the total volume of buildings connected with the Turin network. As shown in the figure this is a looped network.

Two scenarios corresponding with different changes in the thermal request profiles have been analyzed, as reported in Table 2. In both cases it has been considered that only 50% of the buildings accept to modify their thermal request profiles. The two cases differ in terms of the maximum anticipation in the start-up time of the heating system. The energy demand of the selected users has been modified in the following way: 1) a simulation corresponding with a scenario with no changes operated on the thermal request profiles is performed. This simulation allows one obtaining the thermal load curve and the internal temperature in each building as the function of time; 2) the time at which the heating system is switched on is anticipated of a period between 0 and the maximum value indicated in the table; 3) when the indoor temperature of a building reaches a desired value, during the first half of the morning, the heating system is switched off until the internal temperature profile crosses the curve corresponding to the scenario with no changes. For each building, a temperature evolution curve is obtained. This curve is above the original curve in the first part of the morning. When the two curves cross each other, the thermal request profile continues in the same way as the scenario with no changes.

It is important here to stress the fact that the use of an average temperature for the building is not a limitation since the criterion for acceptability of the new request profile is based on the comparison of the curves with and without changes. It is assumed that if the average temperature for the scenario with no changes was acceptable for the end-users, the fact that the same temperature is reached with the new profile guarantees the same comfort conditions.

The modified profile generally involves a larger thermal consumption for the building, nevertheless, this consumption takes place in off-peak hours where cogeneration is available, while it is reduced the thermal request in peak hours. The primary energy cost of these two amounts of heat is thus different: the off-peak heat request has a primary energy production cost of about 0.36 MWh/MWh, while the avoided heat consumption in peak hours has an avoided primary energy cost of about 1.11 MWh/MWh. In fact, cogenerated heat is produced by combined cycles characterized by an electrical efficiency of 58%. When these plants operate in maximum cogeneration mode, electricity production decreases of about 50 MW, while heat production increases of about 240 MW.

Therefore the primary energy cost of a unity of heat production is the same as 0.21 unities of electricity. In contrast, the avoided heat production in peak hours allows reducing the use of industrial boilers which are characterized by an average efficiency of about 90%.

Table 2. User request modification analyzed.

	Fraction	Maximum anticipation
CASE 1	50%	20min
CASE 2	50%	30min

### 3. Results

#### 3.1 Building Model Validation

In this section, results of the building model validation are reported. A specific building where four temperature sensors were installed has been considered. Results in terms of indoor temperature evolution and heat flux measured at the heat exchangers are evaluated and compared with available measurements. In Figure 5, the temperature evolution computed through the building model (in black) is compared to the temperature evolutions measured in four different rooms. A winter day with an average external temperature of 8 °C is considered.

The evolution is well captured by the model both in the heating-on and heating-off stages. During the heating stage the temperature increases of 4.5 degrees, the same of the temperature detected using the thermocouple installed in the building. Also, the time at which the maximum internal temperature is reached in simulations is similar to that occurring in the reality. It is worth noticing that the model does not consider any contribution due to unpredictable contributions, such as solar radiation. This explains the under-prediction of internal temperatures when the heating system is switched on. Nevertheless, it must be remarked the fact that the goal of the model consists in capturing the differences produced by modifying the heating schedule.

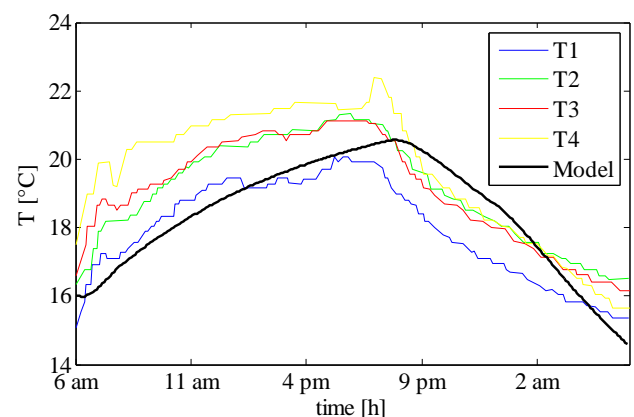


Figure 5. Model validation. Indoor temperature comparison.

Figure 6 illustrates a comparison of the heat request at the heat exchanger evaluated using the building model and the experimental data. It is possible to notice that the heat flux exchanged at the thermal substation is very large when the heating system is switched on. This is due to the fact that temperature on the secondary circuit drops significantly at nights reaching a temperature close to the internal

building temperature. The average temperature difference between primary and secondary side is thus much larger than at design and so the heat flux. After the peak, the heat flux decreases due to the temperature increase on the secondary circuit. This decreasing trend is affected by the characteristic time requested to complete the secondary circuit.

From Figure 6 it can be concluded that the model is able to capture the heat flow evolution at the heat exchanger both in transient and steady state conditions.

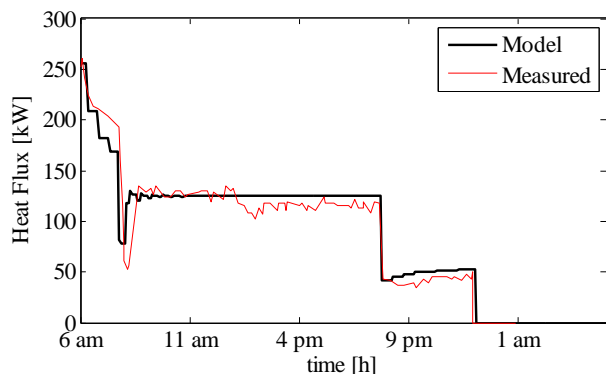


Figure 6. Model validation. Heat request at the heat exchanger comparison.

In addition, six buildings connected with the selected distributed network are considered. For these buildings it is possible to compare the calculated temperature of water exiting the heat exchanger on the primary network with the experimental values. These buildings are also used in the next section in order to show the effects of the rescheduling on the internal temperatures. The criteria to select the buildings are their volume and the distance between the building and the connection node with the transport network. These pieces of information are reported in Table 3, where model coefficients are also shown. These coefficients have been evaluated using the approach described in section 2.1. Last term ( $t_c$ ) is the characteristic time considered in the simulation of each building.

Table 3. User model coefficients.

Building	Volume (m <sup>3</sup> )	Distance (m)	$U_{vol}V$ (W/K)	$Mc$ (kJ/K)	$t_c$ (s)
a	3127	169	3752	70357	150
b	3000	856	2880	69005	150
c	6930	200	6029	169785	320
d	7019	769	5755	176176	300
e	14470	313	10418	393584	560
f	16725	750	19233	460773	660

A comparison between the calculated and measured temperatures of water exiting the selected heat exchangers is shown in figure 7, which shows that the model is able to capture the behavior of buildings, with the exception of building C. In this latter case, the deviation is due to an error in data recording, as confirmed by the wrong value assumed during the morning pause (between 10 a.m. and 12 a.m.) which does not change despite the fact that the heating system is switched off. In contrast the behavior is correctly captured after 4 p.m.

On the basis of the results presented in this section it is possible to conclude that the model is suitable for

evaluating the acceptability, in terms of comfort level, of possible changes in the thermal request.

## 2.2 Current Thermal Request

A first simulation of the distribution network and the buildings connected with the network is performed in order to reconstruct the scenario “as-is”. Thermal request of the buildings is set on the basis of measurements available using a time step of 5 minutes. The peak request of each building together with the time at which it occurs is registered. These pieces of information are illustrated in Figure 8, where the various contributions and the total summation in each timeframe are presented. It is apparent that, as expected, there are many users requiring the highest amount of thermal power between 5.40 am and 6.40 am. The peak thermal power required from most of the buildings is below 1 MW. It can also be noticed that a large user presents a peak thermal request of 2750 MW at 8.45 am, which is an uncommon behavior. This type of user does not need any thermal request variation since its start-up peak occurs when most users are in off-peak conditions.

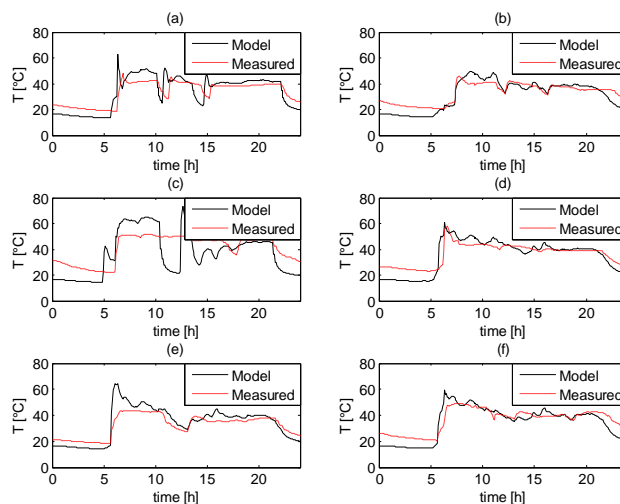


Figure 7. Temperature of water exiting the heat exchanger on the primary side for six selected buildings.

As expected, the peak thermal power presents a maximum at 6.20 am. The peak value obtained in Figure 8 is not the maximum thermal request of the distribution network, because this only accounts for the peak request of each user. Users characterized by earlier peak request may have already reached the pseudo steady-state request, as shown in figure 6, therefore the instant request may be different in shape and values.

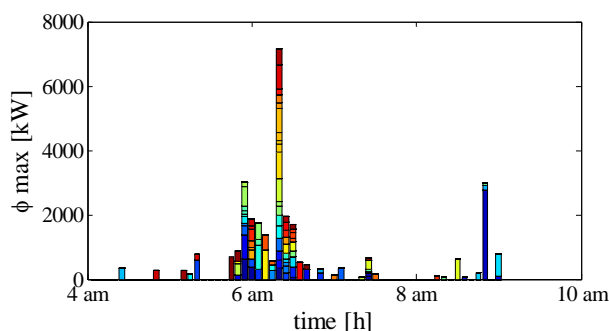


Figure 8. Current situation. Summation of the thermal peaks of the various buildings.

Figure 9 depicts the current total thermal load registered at the end nodes of the distribution network i.e. at the nodes linking the distribution network with the transport network. The thermal request between 0 a.m. and 5 a.m. is close to 0 MW, due to the absence in the considered network of users requiring heat also during the night, i.e. hospitals. A peak load of about 42 MW occurs at about 6.10 a.m., which means about 10 minutes before the maximum value reported in Figure 8. This is mainly due to the shape of the heat flux curves of the buildings, which is typically characterized by a thinner peak than that shown in figure 6 (which refers to a large building) and a slighter increase towards the pseudo steady state.

Then the thermal load reduces to values which vary between 10 MW and 20 MW. The red dashed line, represents the amount of thermal power that can be provided in cogeneration mode to this network. Such value has been obtained by distributing the total cogeneration capacity among the various distribution network according with their specific nominal request. As already discussed in this work, the presence of the morning peak does not allow proper exploitation of the cogeneration plants.

In the following section, possible strategies obtained by modifying the thermal request of the buildings are analyzed.

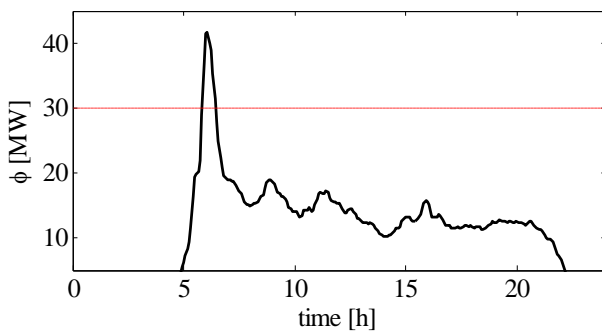


Figure 9 Current thermal power request evolution in the considered distribution network.

### 3.3 Thermal Request Modifications

Two different request profiles that are alternative to the current operational strategy have been defined. The corresponding distributions of peaks are shown in Figure 10. In the first strategy the maximum peak summation is reduced to about 5 MW, but the main variation refers to the anticipation of peaks that in the current strategy occur before 6.10 a.m.: all peaks are made more homogeneous than that shown in figure 8 and are all below 2 MW. In the case of the modified strategy 2, the opportunity to anticipate up to 30 minutes is used to create a sort of alternation between “high” peaks of about 1-2 MW and small peaks.

The time profiles of the total heat load for the distribution network obtained by applying the current operational strategy and two alternative strategies are illustrated in Figure 11. Clearly, when the request of buildings is anticipated the total thermal request presents an anticipated increase. Both modified strategies 1 and 2 provoke a remarkable reduction in the peak load. Before the peaks, the alternative strategies require an additional amount of heat, but this is mainly supplied by cogeneration plants. In contrast, load is reduced after the peak, even if not of the same quantity, therefore a partial heat recovery is obtained. In the case of modified strategy 1, the additional

thermal energy supplied to the network through cogeneration is 0.8 MWh/day, but the avoided production of thermal energy through boilers is about 1.4 MWh/day. This results in a reduction of primary energy consumption of more than 1.2 MWh/day. In the case of the second strategy, the additional thermal energy supplied to the network through cogeneration is about 1.2 MWh/day, but the avoided production of thermal energy through boilers is about 2.5 MWh/day. This results in a reduction of primary energy consumption of more than 2.3 MWh/day.

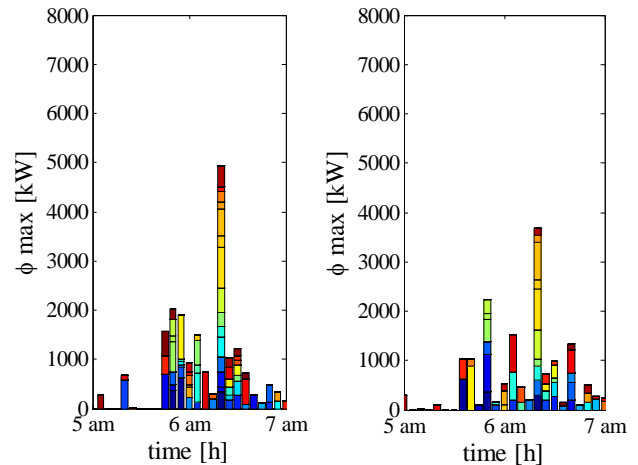


Figure 10. Modified strategies 1 (left) and 2 (right). Summation of the thermal peaks of the various buildings.

If this result is extrapolated to the entire network, assuming that 50% of the request of buildings is rescheduled, the primary energy savings could be about 4-5% of the annual fuel consumption.

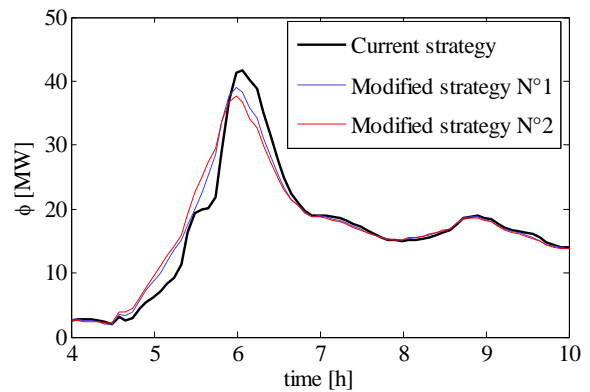


Figure 11 Thermal power request evolution in the considered distribution network with different user request variation strategy.

The analysis of the indoor temperature using the building model is presented in Figure 12 for the six selected buildings. For each building, two curves are shown, corresponding with the current strategy and the modified strategy. Only the strategy 2 is shown, since it is the one involving the largest possible deviation in the startup schedule. In all cases the heating system is stopped at night, therefore internal temperature decreases reaching a minimum at about 5-6 a.m. then the heating system is turned on and the internal temperature start increasing. In the case of building (a) and (c), it is possible to notice that the heating system is stopped during the day (at 10.05 and 10.30, respectively), therefore the average internal temperature calculated using the compact model presents one or more oscillations above 20 °C. In contrast, the other

buildings reach a plateau after an initial steep increase, which involves a reduction in the thermal request in the second part of the morning (after about 10 am) and a modulation during the day.

When the modified strategy is applied, the indoor temperature presents an anticipated increase, therefore the internal temperature curve stays above that corresponding with the current strategy. In the second part of the morning, between 9 and 11 for the examined building, the recovery is applied. This is obtained through partial anticipation of the stop in the case of buildings (a) and (c) or by introducing such stop in the other cases. This stop is calculated so that the indoor temperature curve corresponding with the modified request crosses that corresponding with the current request. From this point on the thermal request profile follows the current one and so the indoor temperature. The fact that the indoor temperature is always maintained above or coincident with that corresponding with the application of the current strategy guarantees the fact that the modified strategies are acceptable for the end-users.

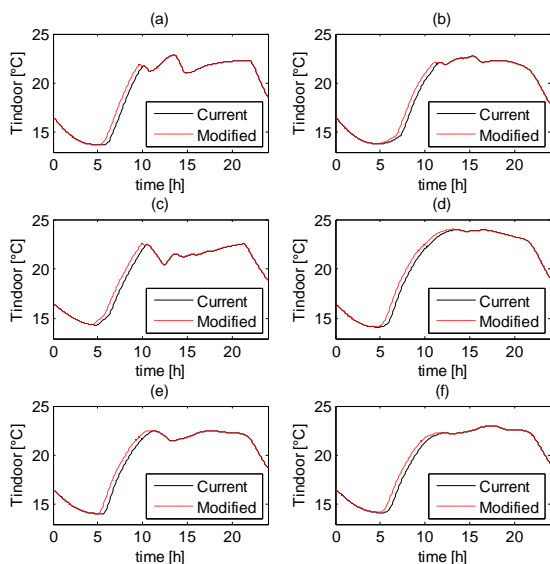


Figure 12. Indoor temperature evolution with the current and the modified users thermal requests.

## Conclusions

In this paper, a simulation approach for the analysis of primary energy savings that can be achieved through rescheduling the thermal request of buildings connected with district heating system is proposed. The effect of these changes is that of a virtual storage that allows reducing peak load in thermal plants and thus increasing the utilization of high efficiency and low carbon heat generation technologies, such as waste heat, cogeneration and renewable. The modeling approach consists of two integrated modules: a district heating model which allows one obtaining the thermal load profile starting from the thermal request profiles of the buildings and a building model, which allows one to obtain the effects of possible rescheduling on the indoor temperatures. The building model is very compact, which permits an easy calibration using experimental data and also the application to a large number of connected buildings. A comparison of the model results with internal temperatures measured in a building and temperatures of water exiting the heat exchanger in six

selected buildings shows that the model is suitable for examining the effects of possible rescheduling.

The simulation tool is applied to a distribution network supplying heat to 105 buildings connected with the Turin district heating system. Results show that the application of rescheduling strategies allows one to reduce the primary energy consumption of up to 2.5 MWh/day through larger use of cogeneration and reduction in the use of boilers. Assuming that the same result per unit volume can be achieved for the other distribution networks, the annual primary energy consumption could be reduced of the order of about 5%.

The analysis of the internal temperatures obtained using the compact building model shows that the same level of comfort can be guaranteed, as the calculated average internal temperatures are always above or coincident with that obtained by applying the current schedule. This means that the rescheduling strategies are able to comply with the end-user requirements.

## Acknowledgements

This work has been conducted within the FP7 Project DIMMER District Information Modeling and Management for Energy Reduction. Small or medium-scale focused research project (STREP) FP7-SMARTCITIES-2013 ICT-2013.6.4 Optimizing Energy Systems in Smart Cities. Authors are very grateful to the technicians of IREN for providing the operation data used in this work.

## Nomenclature

$A$	Incident matrix	
$c$	Thermal Capacity	kJ/kgK
$M$	Mass	kg
$T$	Temperature	K
$U_{vol}$	Thermal losses coefficient	kW/K
$V$	Volume	m <sup>3</sup>
$\Phi$	Heat power	kW

## References:

- [1] H. Lund, B. Moller, B. V. Mathiesen, A. Dyrelund, "The role of district heating in future renewable energy systems," *Energy*, 35, 1381–1390, 2010.
- [2] C. Tripodi: Iren Energia, *Evolution of the Turin District Heating System and the Design of North-West District Network* (In Italian) [Online]. Available: [http://www.fiper.it/fileadmin/user\\_upload/news/energet\\_hica2012/tripodi.pdf](http://www.fiper.it/fileadmin/user_upload/news/energet_hica2012/tripodi.pdf)
- [3] F. Colella, A. Sciacovelli, V. Verda, "Numerical analysis of a medium scale latent energy storage unit for district heating systems," *Energy*, 45, 397-406, 2012
- [4] V. Verda, G. Baccino, "Primary energy reductions in District Heating Networks through variation of the thermal load profile of the users" in *ECOS 2014: Proceedings of The 27th International conference on efficiency, cost, optimization, simulation and environmental impact of energy systems*, Turku, Finland, June 15-19, 2014.
- [5] D. Lindenberger, T. Bruckner, H. M. Groscurth, & R. Kümmel, "Optimization of solar district heating systems: seasonal storage, heat pumps, and cogeneration," *Energy*, 25, 591-608, 2000.

- [6] A. Pini Prato, F. Strobino, M. Broccardo, & L. Giusino, "Integrated management of cogeneration plants and district heating networks," *Applied Energy*, 97, 590-600, 2012.
- [7] V. Verda, & F. Colella, "Primary energy savings through thermal storage in district heating networks," *Energy*, 36, 4278-4286, 2011.
- [8] E. Jokinen, K. Kontu, S. Rinne, R. Lahdelma, "Demand side management in District Heating buildings to optimize the heat production," in *ECOS 2014: Proceedings of The 27th International conference on efficiency, cost, optimization, simulation and environmental impact of energy systems*, Turku, Finland, June 15-19, 2014.
- [9] M. A. Ancona, F. Melino, A. Peretto, "An Optimization Procedure for District Heating Networks," *Energy Procedia*, 6, 278-281, 2014.
- [10] M. Bojic, N. Trifunovic, "Linear programming optimization of heat distribution in a district-heating system by valve adjustments and substation retrofit," *Building and Environment*, 35, 151-159, 2000.
- [11] F. Harary, *Graph Theory*, New Delhi: Narosa Publishing House, 1995.
- [12] S. V. Patankar, *Numerical Heat Transfer and Fluid Flow*, New York: Taylor & Francis, 1980.
- [13] J. H. Ferziger, M. Peric, *Computational Methods for Fluid Dynamics, 3rd Ed.*, Berlin: Springer, 2001.
- [14] A. Sciacovelli, V. Verda, R. Borchiellini, *Numerical Design of Thermal Systems*, Torino: Clut, 2015
- [15] E. Guelpa, A. Sciacovelli, V. Verda, "Thermo-fluid Dynamic Model of Complex District Heating Networks for the Analysis of Peak Load Reductions in the Thermal Plants" *Proceedings of ASME IMECE*, Houston, Texas, 2015, Paper No. IMECE2015-52315